2007

Single-crystal growth and anisotropic magnetic properties of nonstoichiometric three-layer sodium cobalt oxides

Dapeng Chen
University of Wollongong, dapeng@uow.edu.au

Xiaolin Wang
University of Wollongong, xiaolin@uow.edu.au

C T Lin
Max Planck Institute for Solid State Research, Germany

S X. Dou
University of Wollongong, shi@uow.edu.au

Publication Details

Chen, D, Wang, X, Lin, C & Dou, SX (2007), Single-crystal growth and anisotropic magnetic properties of nonstoichiometric three-layer sodium cobalt oxides, Physical Review B (Condensed Matter and Materials Physics), 76, pp. 134511-1-134511-6.

Single-crystal growth and anisotropic magnetic properties of nonstoichiometric three-layer sodium cobalt oxides

Abstract

Large single crystals of α-Na_xCoO_2 (x=0.91, 0.92, and 0.93) have been successfully fabricated by using the traveling solvent floating zone method. Details on the crystal growth are discussed. The crystal structures were characterized using powder x-ray diffraction and Rietveld refinement. The magnetic susceptibility measurements show that the magnetic properties depend strongly on x. The compound was found to be antiferromagnetic at $T_N \approx 20$ K for x=0.91 and x=0.92, and paramagnetic for x=0.93. The in-plane and out-of-plane anisotropies were observed for the x=0.91 crystals. In addition, the derived anisotropic g-factor ratios (g_{ab}/g_c) from the anisotropic susceptibility along H||ab and H||c decreased significantly as the sodium composition increased from x=0.91 to x=0.93.

Keywords

Single, crystal, growth, anisotropic, magnetic, properties, nonstoichiometric, three, layer, sodium, cobalt, oxides

Disciplines

Engineering | Physical Sciences and Mathematics

Publication Details

Chen, D, Wang, X, Lin, C & Dou, SX (2007), Single-crystal growth and anisotropic magnetic properties of nonstoichiometric three-layer sodium cobalt oxides, Physical Review B (Condensed Matter and Materials Physics), 76, pp. 134511-1-134511-6.

Single-crystal growth and anisotropic magnetic properties of nonstoichiometric three-layer sodium cobalt oxides

D. P. Chen,[1,2] Xiaolin Wang,[1,*] C. T. Lin,[2] and S. X. Dou[1]
[1]*Institute for Superconducting and Electronic Materials, University of Wollongong, New South Wales 2500, Australia*
[2]*Max Planck Institute for Solid State Research, Heisenbergstrasse 1, D-70569 Stuttgart, Germany*
(Received 25 July 2006; revised manuscript received 19 May 2007; published 19 October 2007)

Large single crystals of α-Na_xCoO_2 (x=0.91, 0.92, and 0.93) have been successfully fabricated by using the traveling solvent floating zone method. Details on the crystal growth are discussed. The crystal structures were characterized using powder x-ray diffraction and Rietveld refinement. The magnetic susceptibility measurements show that the magnetic properties depend strongly on x. The compound was found to be antiferromagnetic at $T_N \approx 20$ K for x=0.91 and x=0.92, and paramagnetic for x=0.93. The in-plane and out-of-plane anisotropies were observed for the x=0.91 crystals. In addition, the derived anisotropic g-factor ratios (g_{ab}/g_c) from the anisotropic susceptibility along $H \| ab$ and $H \| c$ decreased significantly as the sodium composition increased from x=0.91 to x=0.93.

DOI: 10.1103/PhysRevB.76.134511 PACS number(s): 74.62.Bf, 61.10.−i, 74.25.Ha, 75.30.Gw

I. INTRODUCTION

Since the discovery of simultaneous surprisingly high thermoelectric power and low resistivity in Na_xCoO_2 ($x \leqslant 1$),[1,2] and in particular, the discovery of superconductivity at temperatures below 5 K in $Na_{0.35}CoO_2.1.3H_2O$, which is formed by the deintercalation of Na from double layer γ-Na_xCoO_2 followed by a full hydration process,[3] these materials have attracted considerable interest.

Early investigations on the sodium-cobalt-oxygen system have revealed that crystals with the formula Na_xCoO_2 ($x \leqslant 1$) are bronze type phases, consisting of sheets of octahedra $(CoO_2)_n$ between which are inserted sodium ions.[4] The unit cell of γ-Na_xCoO_2 has a $P2$ structure (prismatic, two layer), i.e., with two sheets of edge shared CoO_2 in its unit cell, which are rotated by 60° with respect to each other. The sodium ions, on two crystallographically distinct sites, are trigonal prismatic (P) in coordination to the oxygen atoms. α-Na_xCoO_2 has an $O3$ structure (octahedral, three layer), i.e., has three sheets of edge shared CoO_2 per unit cell, displaced laterally from each other. The sodium ions are located only on one crystallographic site in an octahedron (O), with coordination to the oxygen atoms.

The transport and magnetic properties of two-layer Na_xCoO_2 are strongly dependent on the Na content. It has been found that as x increases from 0.3, the ground state of these compounds goes from a paramagnetic metal through a charge ordered insulator (at x=0.5) to a "Curie-Weiss metal" (around x=0.70), and finally, to a weak-moment magnetically ordered state ($x > 0.75$).[5] Muon spin rotation and NMR measurements have identified the stoichiometric three-layer Na_1CoO_2 phase to be a nonmagnetic insulator.[6,7]

No superconductivity has been found in a new series of sodium cobalt oxyhydrates obtained from the parent compound β-$Na_{0.6}CoO_2$,[8] whereas the sodium cobalt oxyhydrates formed from α-$NaCoO_2$ show superconducting transitions at 4.3–4.6 K.[9,10] Both parent materials have three CoO_2 layers per unit cell, in contrast to the first superconductor, $Na_xCoO_{2\cdot y}H_2O$, which was obtained from a parent γ-Na_xCoO_2 containing only two CoO_2 layers per unit cell. This indicates that the geometrical shape of the site for the Na ions and the number of CoO_2 sheets play an important role in the resultant electronic and magnetic properties.

Single crystals are very desirable for experiments that require large volumes or areas of samples, such as neutron diffraction and anisotropic property measurements. Data obtained from the single-crystal samples will shed light on the electronic and structural properties of this new type of superconductor. There has been much research on this family of materials. Single-crystalline whiskers with x=0.5 have been grown by an unconventional method from potassium-containing compositions. The maximum size of the whiskers is 1.6 mm in length, 15–40 μm in width, and 1.5–4.0 μm in thickness.[11] Using NaCl as a flux, platelike single crystals of $NaCo_2O_4$ and $NaCoO_2$ have been prepared with typical sizes of $1.5 \times 1.5 \times 0.03$ mm^3 and $0.5 \times 0.5 \times 0.02$ mm^3, respectively.[1,12–14] Compared to these methods, the traveling solvent floating zone (TSFZ) method is just as suitable for such single-crystal growth. In principle, crystal growth can be performed continuously at one point on the temperature-composition phase diagram. Chou *et al.* succeeded in growing large single crystals of two-layer Na_xCoO_2 from a feed rod with x=0.75 using an optical floating zone furnace under oxygen atmosphere.[15] Single crystals of Na_xCoO_2 with nominal Na content from 0.50 to 1.00 have also been grown successfully using the TSFZ method.[16–18] In this contribution, we present a detailed study on the crystal growth of large and high quality three-layer Na_xCoO_2 (x=0.91, 0.92, and 0.93) single crystals by the floating zone method and demonstrate their structural behavior and anisotropic magnetic properties.

II. EXPERIMENT

The feed rods for the crystal growth were prepared by the conventional solid-state method. Powders of Na_2O_2 (97%) and Co_3O_4 (99.998%) were mixed in the molar ratios Na:Co=1.00:1.00, 1.05:1.00, and 1.10:1.00 in an argon filled glovebox. The temperature was slowly (150 °C/h) increased to 850 °C, held constant for 24 h, and, finally,

slowly cooled down to room temperature in flowing oxygen. The polycrystalline powders were reground and formed into cylindrical rods 7 mm in diameter and 80 mm in length in an argon filled glovebox. The rods were hydrostatically pressed under a pressure of ~70 MPa and then sintered at 900 °C for 24 h in flowing oxygen. After sintering, a 20 mm long rod was cut to serve as the first seed for crystal growth.

The crystal growth was performed in an infrared radiation furnace equipped with four 300 W halogen lamps. Prior to the crystal growth, a high density feed rod (~90% of the crystal density) was obtained by premelting the rod at the rapid rate of 25 mm/h in flowing oxygen. A short polycrystalline premelted feed rod (~20 mm in length) was used as the seed rod in the crystal growth. Trials were made in which crystals were grown in different atmospheric compositions and pressures as follows: flowing oxygen, flowing argon, and low oxygen pressure (2 atm). The crystal growth speed also varied between 1 and 5 mm/h accompanied by a counter-rotation of the feed and seed rods at 30 rpm to ensure efficient mixing of the liquid and uniform temperature distribution in the molten zone.

Crystal wafers were cut perpendicular to the growth direction and polished to a mirror finish to allow us to examine them for the existence of macroscopic defects such as cracks and twins, grain boundaries, and inclusions under a polarized microscope. Compositional analysis of the as-grown crystals was obtained from induction-coupled plasma atomic emission spectroscopy (ICP-AES). A Mo $K\alpha$ x-ray source was used for powder x-ray diffraction (XRD) measurements to check the phase purity and the crystal structure.

Single-crystal XRD was carried out on mechanically cleaved faces of the crystals along the growth direction to examine the crystalline quality and orientation of the crystal growth. The measurements were conducted in a θ-2θ scan mode in the 2θ range of 10°–120° for single-crystal measurements. Cu $K\alpha$ radiation was used as x-ray source.

The magnetic susceptibility measurements were carried out using a superconducting quantum interference device magnetometer (Quantum Design, model MPMS 7.0) over the large temperature range of 2–350 K. Magnetic fields were perpendicular and parallel to the c axis for cleaved as-grown crystals.

III. RESULTS AND DISCUSSION

A. Crystal growth

When preparing the polycrystalline Na_xCoO_2 by the solid-state method, sintering the feed rods, premelting the feed rods, and growing the crystals at high temperatures, the sodium loss caused by high Na_2O vapor pressure should be considered. Therefore, ceramic powders were synthesized using additional Na_2O_2 for compensation. Sintered powders were observed by XRD to consist of a main phase of α-$NaCoO_2$ with little Co_3O_4 impurity mixture, due to the slow reaction in the core of the rod compared to the outside area; this is what normally happens in this series of compounds. Crystals grown using the impure feed rod did not contain any impurities since Na has a large solubility range in the α phase in this system, and the Na loss is corrected by homogeneous mixing in the following molten process.

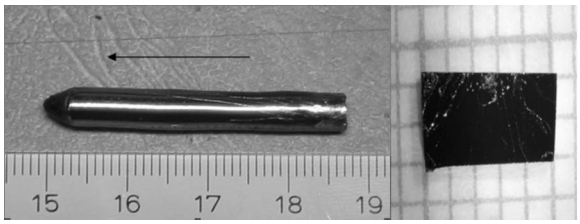

FIG. 1. (Left) As-grown single crystal of α-$NaCoO_2$ and (right) the cleaved crystal from the last grown part of the ingot.

Crystals grown under different conditions follow the aforementioned procedures. The quality of the premelted feed rods is one of the critical conditions of the TSFZ technique, because during the crystal growth the molten zone is sustained by the feed rod through surface tension. A straight, long, and equal-diameter feed rod is required to stabilize the molten zone over a long growth period. We found that it was very difficult to stabilize the molten zone during the atmospheric flow, due to the evaporation of Na, which can be observed as white Na_2O deposited on the inner wall of the quartz tube, with the molten zone collapse being the result of the composition change. Application of low-pressure oxygen (2 atm) during growth was found to greatly reduce the Na evaporation. Under these conditions, zone travel rates of 1.0, 2.0, 3.0, and 5.0 mm/h were employed. It was found that the zone travel rates in this range have no detectable influence on the crystal quality. However, we observed that the slower rate stabilized the molten zone. Considering the evaporation of Na ions during the growth, much slower rates were not applied.

Figure 1(a) presents a typical α-Na_xCoO_2 boule, which was grown at the moderate rate of 2 mm/h under an oxygen pressure of 2 atm in an attempt to reduce the volatilization of Na and obtain large crystals. The boule was black with a metallic luster, and was 5 mm in diameter and 37 mm in length. The arrow indicates the crystal growth direction. Due to the layer growth mechanism, the crystal grains were found to grow preferentially along the crystallographic *ab* plane, parallel to the rod axis. It was found that the cleaved surface of the as-grown crystal was shiny, but unstable under atmospheric conditions, in contrast to γ-phase Na_xCoO_2 crystal. The cleaved surface became dull just 20 min after cleavage due to its reaction with moisture and CO_2 in the air. The crystal samples must be quickly removed after processing and stored in a clean and dry container to prevent the absorption of moisture.

The crystal wafers were cut from the last grown part and polished to a mirror finish. Under a polarized light microscope, only a few separate grains were found in the peripheral area. No inclusions, cracks, or grain boundaries were observed in the inner area of about 4 mm diameter. Figure 1(b) displays a crystal with dimensions up to $5\times2\times1$ mm^3, which was mechanically cleaved from the central region of the last grown part of the ingot with a sharp steel pin.

B. Composition and structure

There can be a concentration gradient of Na either along or across the crystal growth direction. In order to minimize

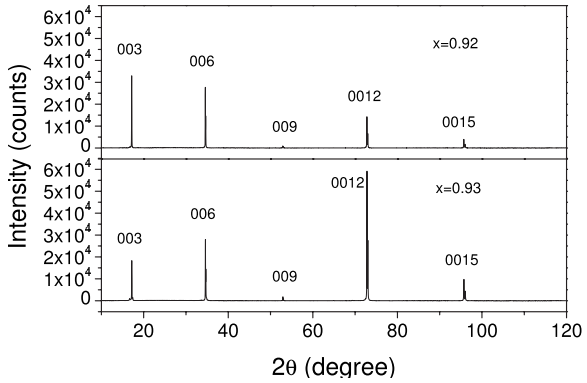

FIG. 2. X-ray diffraction patterns for α-$NaCoO_2$ single crystals cleaved along the growth direction. All the peaks can be attributed to (00l).

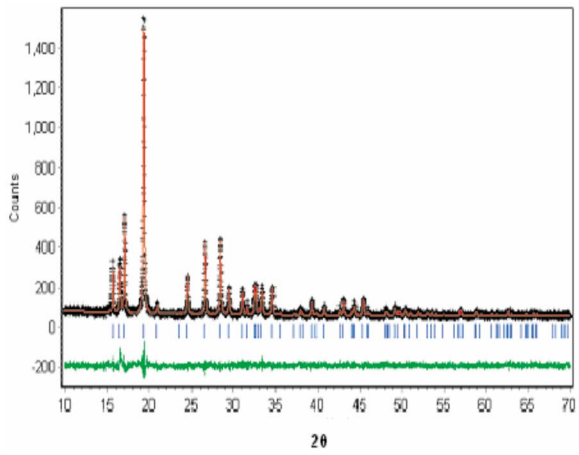

FIG. 3. (Color online) Rietveld refinement pattern for the as-grown α-$Na_{0.92}CoO_2$ crystal. The observed diffraction intensities and the calculated patterns are represented by plus signs and solid lines, respectively. The curves at the bottom represent the difference. Short bars below the observed and calculated patterns indicate the positions of allowed Bragg reflections.

this possibility, the crystal wafers were cut from the last grown part in the range of 2–3 mm from the end. Three pieces of crystal were cut from the same crystal wafer, and all three pieces were analyzed by ICP-AES. We found that the Na concentrations of the three pieces of crystal are very close. The average values of Na determined from the three pieces of crystal are $x=0.91$, 0.92, and 0.93 for the starting compositions of $Na_{1.00}CoO_2$, $Na_{1.05}CoO_2$, and $Na_{1.10}CoO_2$, respectively. Single-crystal XRD measurements were made on both as-grown crystals. Platelike crystals were cleaved along the growth direction. Typical XRD patterns are shown in Fig. 2. All the peaks were indexed to be the (001) peaks of α-$NaCoO_2$. Using a fitting method with the Nelson-Riley (NR) function, the c-axis lattice constant is estimated to be 15.597(2) Å for $Na_{0.92}CoO_2$ and 15.5928(9) Å for $Na_{0.93}CoO_2$. No traces of impurities or inclusions were observed in our samples.

The structure refinement of $Na_{0.92}CoO_2$ was performed using a Rietveld analysis program. We adopted the space group R-3m and assumed that the sodium ions are on the (0, 0, 0) site and are coordinated octahedrally to the oxygen from the CoO_2 layers. Table I lists the refined structure parameters, and Fig. 3 presents the refinement pattern of the $Na_{0.92}CoO_2$ single crystal. The final factors were low enough, decreasing to $R_p=8.50\%$, $R_{wp}=10.89\%$, $R_B=1.83\%$, and $\chi^2=1.01$. The cell parameters are $a=2.887\ 62(17)$ Å and $c=15.6020(8)$ Å. The lattice parameters of $Na_{0.93}CoO_2$ were determined by single-crystal x-ray diffraction along (0, 0, l) and $(h,k,0)$ at room temperature, resulting in values of $a=2.8878(7)$ Å and $c=15.596(2)$ Å; these values agree with the reported crystal data of α-$NaCoO_2$.[14,19]

C. Magnetic anisotropy

The temperature dependence of the susceptibility for the $Na_{0.92}CoO_2$ sample, as measured in a field of 1 T oriented either along or perpendicular to the (001) direction, is shown in Fig. 4. Upon cooling, a peak develops around 20.5 K, which is sharper than that observed in two-layer $Na_{0.82}CoO_2$ single crystal.[20] The following sharp decrease of the (001) direction susceptibility around 19.6 K heralds an antiferromagnetic transition with ordered moments along c. The inset in Fig. 4 shows that the transition is only weakly affected by the field. The upturn of the curves below 14 K appears to be due to paramagnetic contributions from impurities; this upturn is suppressed in a field of 5 T.

The magnetization is very sensitive to the presence of Co_3O_4 and CoO, which are antiferromagnets with $T_N=35$ and 292 K, respectively. No other transitions in the susceptibility have been found from 20.5 K to room temperature for any of the samples, indicating high quality of the single-crystal samples. This is consistent with x-ray diffraction measurements, which exhibit no traces of impurities.

The temperature dependence of the susceptibility for the $Na_{0.93}CoO_2$ sample measured in a field of 1 T parallel and perpendicular to the (001) direction is shown in Fig. 5. It can be seen that the antiferromagnetic transition at 19.6 K seen in the $Na_{0.92}CoO_2$ sample is absent for the $Na_{0.93}CoO_2$

TABLE I. Crystallographic data for $Na_{0.92}CoO_2$ in the space group R-3m (No. 166).

Atom	Wyckoff position	x	y	z	Occupancy	Biso (Å)[a]
Na	3a	0	0	0	0.919(2)	0.98(9)
Co	3b	0	0	0.5	1	0.57(7)
O	6c	0	0	0.2308(3)	1	0.52(10)

[a]Isotropic temperature factor.

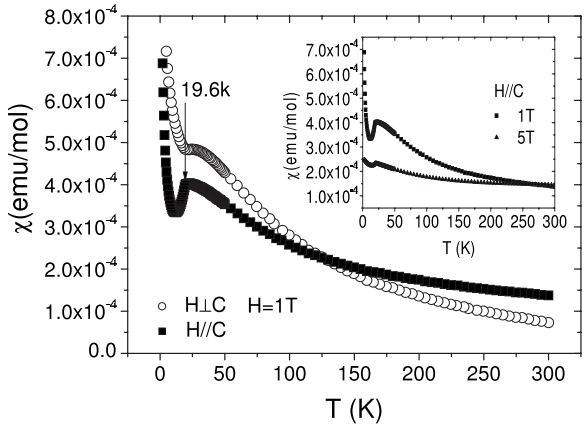

FIG. 4. Temperature dependence of the susceptibility for $Na_{0.92}CoO_2$ sample measured with field parallel and perpendicular to the (001) direction. Inset shows the data measured in 1 and 5 T with field parallel to (001).

sample. Furthermore, χ gradually increases with decreasing temperature, showing typical paramagnetic behavior. The inset figure shows the separation below $T_c \approx 20$ K, where the susceptibility decreased as the applied magnetic field increased below this temperature.

As to why such a little difference in the composition could cause a big difference in the magnetic properties of the α-$NaCoO_2$ single crystals, we believe that the compositions of $x=0.92$ and 0.93 just locate at a boundary (in a magnetic phase diagram) that separates two different regions with different magnetic phases, antiferromagnetic and paramagnetic. Considering the fact that the α phase only forms for $x=0.9$ up to $x=1.0$,[4] the compounds with $x=0.90$ and 0.92 are antiferromagnetic as what have been observed in crystals grown by the flux method[21] and in our crystals presented in this work. For $x>0.92$, samples are paramagnetic (as in the case of $x=0.93$ of our crystals) and eventually become nonmagnetic for $x=1$.[6]

In order to analyze the T dependence of the anisotropic susceptibility quantitatively, we plotted $\chi_{ab}(T)$ versus $\chi_c(T)$

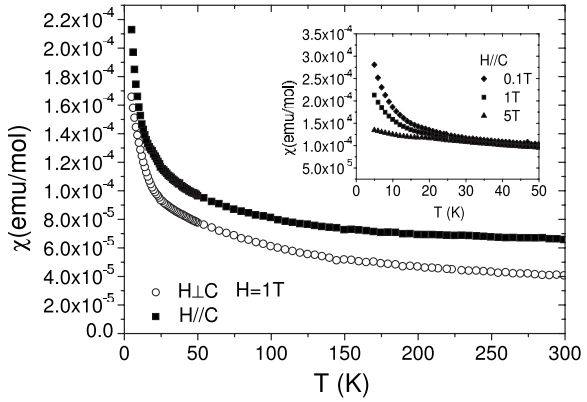

FIG. 5. Temperature dependence of susceptibility for $Na_{0.93}CoO_2$ sample measured in a field of 1 T. The open and closed symbols are for the magnetic field applied perpendicular and parallel to the (001) direction, respectively. Inset shows low temperature results at different parallel magnetic fields.

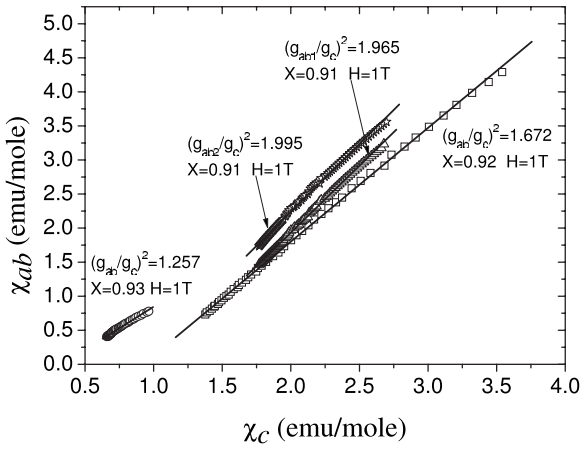

FIG. 6. χ_{ab} versus χ_c for α-Na_xCoO_2 with $x=0.91$, 0.92, and 0.93.

with an implicit parameter T for both single crystals (Fig. 6). The analysis mentioned in Ref. 22 leads to the relation between $\chi_{ab}(T)$ and $\chi_c(T)$:

$$\chi_{ab}(T) = (g_{ab}/g_c)^2 \chi_c(T) + [\chi_0^{ab} - (g_{ab}/g_c)^2 \chi_0^c]$$

The fitted slope of the data in Fig. 6 corresponds to the ratio (g_{ab}/g_c).[2] The samples with $x=0.91$, 0.92, and 0.93 have $g_{ab}/g_c \approx 1.40$, 1.29, and 1.12, respectively. These results indicate that the derived anisotropic g-factor ratios (g_{ab}/g_c) decrease significantly with a little change in sodium concentration, indicating that the physical properties of the three-layer Na_xCoO_2 should be very sensitive to the Na contents.

We fit the temperature dependence of the susceptibility under a 1 T field for the $x=0.91$, 0.92, and 0.93 single crystals to a modified Curie-Weiss law, $\chi=\chi_0+C/(T-\theta)$, by the least-squares calculation, where χ_0, C, and θ are the temperature independent susceptibility, the Curie constant, and the asymptotic Curie temperature, respectively. The fitting parameters for both field orientations in the range $T=50-300$ K are given in Table II. The fitted values for the

TABLE II. Summary of magnetic data for three-layer Na_xCoO_2.

Na_xCoO_2	Field orientations	C (cm^3 K/mol)	θ (K)	χ_0 (emu/mol_{Co} Oe)
$x=0.91$	$\|ab1$	0.0370(6)	−64(2)	−0.00001
	$\|ab2$	0.0491(7)	−85(2)	0.00002
	$\|c$	0.0144(3)	−38(2)	0.00012
x=0.92	$\|ab$	0.0633(14)	−68(2)	−0.0001
	$\|c$	0.0328(6)	−55(2)	0.00004
$x=0.93$	$\|ab$	0.0056(1)	−53(2)	0.00002
	$\|c$	0.00263(9)	−15(2)	0.00006
$x=0.91$ (powder)		0.0334(7)	−63(2)	0.00005
$x=0.92$ (powder)		0.053(1)	−65(2)	−0.00005
$x=0.93$ (powder)		0.0047(1)	−34(2)	0.00005

powder average are also listed. As expected, we find that the Curie constants for $H \| ab$ and $H \| c$ are significantly different for these single-crystal samples, which may arise from an anisotropic g factor. The negative θ suggests antiferromagnetically interacting spins.

The three-layer Na_xCoO_2 has a hexagonal crystal structure with in-plane and out-of-plane parameters $a=2.887$ Å and $c=15.60$ Å, with space group $R\text{-}3m$. It is obvious that the crystal structure is highly anisotropic. Therefore, the difference in the in-plane and out-of-plane magnetic properties is expected, and it has been, indeed, observed in our crystal samples. However, the occurrence of in-plane anisotropy seems hard to predict. Nevertheless, we have noticed that an in-plane anisotropy in two-layer Na_xCoO_2 compounds has just recently been observed using the neutron diffraction technique.[23] Therefore, there could be a possibility of in-plane anisotropy in our three-layer Na_xCoO_2 crystals.

Although the determination of the a direction in the ab plane is very difficult for the Na_xCoO_2 crystals, we can determine how the magnetization changes when magnetic field is rotated in the ab plane. Therefore, the ab in-plane magnetic anisotropy is measured by the following procedures for our crystals: we first measured our sample with the field along one direction in the ab plane (the $ab1$ direction as indicated in the inset of Fig. 7), then measured again by rotating the sample 90° in the ab plane as indicated by the $ab2$ direction in the same inset. A large crystal ($4\times4\times1$ mm^3) with $x=0.91$ was chosen for the in-plane anisotropy study, and its out-of-plane anisotropy was also measured.

The temperature dependence of the susceptibility (χ-T) for the $x=0.91$ sample which was measured in the field of 1 T is shown in Fig. 7. It can be seen that although the susceptibilities measured along the two in-plane directions show the same trend with temperatures, they have about 10%–18% difference in magnitude over a wide range of temperatures. The two in-plane susceptibilities are very different from that along the c direction. A crossover is clearly seen at 120 or 180 K, respectively, which is also seen in the $x=0.92$ sample at 120 K, as shown in Fig. 4. The above results indicate that the in-plane anisotropy exists in the α-phase Na_xCoO_2 crystals. The in-plane and out-of-plane Curie constants are calculated by fitting to the modified Curie-Weiss law, and their values are given in Table II. It can be seen that the C values for the $ab1$ and $ab2$ in-plane directions are very close (0.037 and 0.049). However, the difference between the in-plane and out-of-plane Curie constants is big, which is similar to what has been obtained for the $x=0.92$ and 0.93 crystals. The difference in the in-plane Curie constants is apparently due to the in-plane anisotropy of the three-layer α-phase Na_xCoO_2 crystals. Our observation on the in-plane anisotropy in the α-$NaCoO_2$ single-crystal samples is in agreement with what has been reported for two-layer γ-Na_xCoO_2 phase.[23] However, we point out that it is very hard to align the crystal in the ab plane perfectly for each measurement. Therefore, the less accurate alignment of the ab plane could also contribute to the difference in the susceptibilities in the ab plane. Further work is needed for the in-plane anisotropy measurement with very accurate alignment in the ab plane.

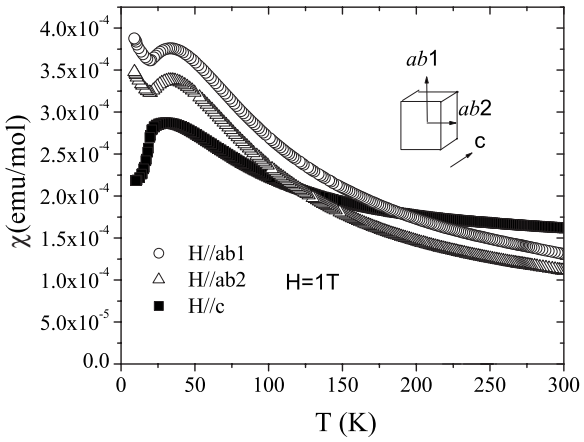

FIG. 7. Temperature dependence of the susceptibility for $Na_{0.91}CoO_2$ sample measured with three different magnetic field directions.

IV. CONCLUSIONS

In summary, large, nonstoichiometric α-Na_xCoO_2 high quality single crystals can be grown using the TSFZ method under oxygen atmosphere. As-grown single crystals are more sensitive under ambient conditions compared with two-layer crystals. The structure derived from the single crystals agrees with the reported powder samples. The lattice parameter c decreases with increasing Na content, while a remains constant. The compound was found to be antiferromagnetic at $T_N \approx 20$ K for $x=0.91$ and 0.92, and paramagnetic for $x=0.93$. The in-plane and out-of-plane anisotropies were observed for the $x=0.91$ crystals. The anisotropic g-factor ratios (g_{ab}/g_c) along $H \| ab$ and $H \| c$ decrease significantly as the sodium composition is slightly increased.

ACKNOWLEDGMENTS

We would like to thank J. Strempfer for measuring the XRD of a crystal and E. Brücher, G. Götz, and Cristal Busch for technical support. This work was partly supported by a Discovery Project from the Australian Research Council.

*Author to whom correspondence should be addressed; xiaolin@uow.edu.au

[1] I. Terasaki, Y. Sasago, and K. Uchinokura, Phys. Rev. B **56**, R12685 (1997).
[2] T. Motohashi, M. Karppinen, and H. Uamauchi, Proceedings of 2002 MRS Fall Meeting, Boston, MA, 2–6 December 2002 (unpublished).
[3] K. Takada, H. Sakurai, E. Takayama-Muromachi, F. Izumi, R. A. Dilanian, and T. Sasaki, Nature (London) **422**, 53 (2003).
[4] C. Fouassier, G. Matejka, F.-M. Reau, and P. Hagenmuller, J. Solid State Chem. **6**, 532 (1973).
[5] M. L. Foo, Y. Wang, S. Watauchi, H. W. Zandbergen, T. He, R. J. Cava, and N. P. Ong, Phys. Rev. Lett. **92**, 247001 (2004).
[6] G. Lang, J. Bobroff, H. Alloul, P. Mendels, N. Blanchard, and G. Collin, Phys. Rev. B **72**, 094404 (2005).
[7] C. de Vaulx, M.-H. Julien, C. Berthier, M. Horvatic, P. Bordet, V. Simonet, D. P. Chen, and C. T. Lin, Phys. Rev. Lett. **95**, 186405 (2005).
[8] Sundip Mistry, Donna C. Arnold, Chris J. Nuttall, Alexandros Lappas, and Mark A. Green, Chem. Commun. (Cambridge) **2004**, 2440.
[9] K. Takada, H. Sakurai, E. Takayama-Muromacki, F. Izumi, R. A. Dilanian, and T. Sasaki, Adv. Mater. (Weinheim, Ger.) **16**, 1901 (2004).
[10] M. L. Foo, T. Klimczuk, Lu Li, N. P. Ong, and R. J. Cava, Solid State Commun. **133**, 407 (2005).
[11] G. Peleckis, T. Motohashi, M. Karppinen, and H. Yamauchi, Appl. Phys. Lett. **83**, 5416 (2003).
[12] K. Fujita, T. Mochida, and K. Nakamura, Jpn. J. Appl. Phys., Part 1 **40**, 4644 (2001).
[13] Masashi Mikami, Masashi Yashimura, Yusuke Mori, Takatomo Sasaki, Ryoji Funahashi, and Masahiro Shikano, Jpn. J. Appl. Phys., Part 1 **42**, 7383 (2003).
[14] Yasuhiko Takahashi, Yoshito Gotoh, and Junji Akimoto, J. Solid State Chem. **172**, 22 (2003).
[15] F. C. Chou, J. H. Cho, P. A. Lee, E. T. Abel, K. Matan, and Y. S. Lee, Phys. Rev. Lett. **92**, 157004 (2004).
[16] D. P. Chen, H. C. Chen, A. Maljuk, A. Kulakov, H. Zhang, P. Lemmens, and C. T. Lin, Phys. Rev. B **70**, 024506 (2004).
[17] D. Prabhakaran, A. T. Boothroyd, R. Coldea, and N. R. Charnley, J. Cryst. Growth **271**, 74 (2004).
[18] C. T. Lin, D. P. Chen, A. Maljuk, and P. Lemmens, J. Cryst. Growth **292**, 422 (2006).
[19] L. Viciu, J. W. G. Bos, H. W. Zandbergen, Q. Huang, M. L. Foo, S. Ishiwata, A. P. Ramirez, M. Lee, N. P. Ong, and R. J. Cava, Phys. Rev. B **73**, 174104 (2006).
[20] S. P. Bayrakci, C. Bernhard, D. P. Chen, B. Keimer, R. K. Kremer, P. Lemmens, C. T. Lin, C. Niedermayer, and J. Strempfer, Phys. Rev. B **69**, 100410 (2004).
[21] Hiroya Sakurai, Satoshi Takenouchi, Naohito Tsujii, and Eiji Takayama-Muromachi, J. Phys. Soc. Jpn. **73**, 2081 (2004).
[22] F. C. Chou, J. H. Cho, and Y. S. Lee, Phys. Rev. B **70**, 144526 (2004).
[23] L. M. Helme, A. T. Boothroyd, R. Coldea, D. Prabhakaran, A. Stunault, G. J. McIntyre, and N. Kernavanois, Phys. Rev. B **73**, 054405 (2006).